ISSN: 1410-8917
Jurnal Kimia Sains & Aplikasi
e-ISSN: 2597-9914

Jurnal Kimia Sains dan Aplikasi 28 (3) (2025): 106-114

Jurnal Kimia Sains dan Aplikasi
Journal of Scientific and Applied Chemistry

Journal homepage: http://ejournal.undip.ac.id/index.php/ksa

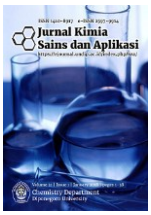

Synthesis, Structure, Hirshfeld Surface Analysis, and Antibacterial Activity of [Ni(3-NH_2py)$_4Cl_2$] Complex (3-NH_2py = 3-aminopyridine)

Putri Dwi Lestari [1], Nani Farida [1], I Wayan Dasna [1,*]

[1] Department of Chemistry, Faculty of Sciences and Mathematics, State University of Malang, Malang, Indonesia

* Corresponding author: idasna@um.ac.id

https://doi.org/10.14710/jksa.28.3.106-114

Article Info

Article history:

Received: 10th November 2024
Revised: 05th March 2025
Accepted: 06th March 2025
Online: 30th April 2025

Keywords:
Ni(II) complex; 3-aminopyridine; crystal structure; Hirschfeld surface; hydrothermal

Abstract

Complex [Ni(3-NH_2py)$_4Cl_2$] was successfully synthesized through the reaction between $NiCl_2.6H_2O$ with 3-NH_2py ligand with a mole ratio of 1:4 using the hydrothermal method at 120°C for 4 hours. The complex was characterized using the melting point test, electrical conductivity, FT-IR, and SC-XRD. The complex compound decomposed at 215°C. Typical absorption bands of 3-NH_2py ligand appeared in the FT-IR spectrum of the complex at wave numbers 3375, 3323, 1585, and 1303 cm^{-1}, indicating the presence of -NH_{as}, -NH_s, C=N, and -C-NH_2 functional groups. The complex compound is an ionic compound that crystallizes in a distorted octahedral structure with a triclinic crystal system and space group $P\bar{1}$ (a = 7.6428(8) Å, b = 8.5384(8) Å, c = 9.8610(13) Å and α = 73.920(4)°, b = 70.149(3)°, g = 71.036(2)°). The *R-factor* value is 4.48%, which shows the refinements are very close to the original structure. Based on the Hirshfeld surface analysis, the intermolecular interaction of N-H···Cl occurs between the H atom of the amine group and the ligand Cl in another molecule. Antibacterial activity tests against *S. aureus* and *E. coli* using chloramphenicol as a positive control. The results showed the inhibition zone diameters for both bacteria were 6.90 mm, higher than that of their free ligand.

1. Introduction

Aminopyridine (NH_2py) is one of the six-membered heterocyclic compounds extensively studied in recent years [1]. NH_2py-based complex compounds have special attention due to their potential as antibacterial agents [2, 3, 4], photocatalytic degradation [5], magnetic properties [6], and catalyst [7]. NH_2py has three isomers: 2-NH_2py, 3-NH_2py, and 4-NH_2py [1]. Most x-NH_2py ligands act as monodentate ligands through the nitrogen donor atom in the pyridine ring, forming monomer complexes in their coordination mode [8, 9, 10]. However, in the complex [M(μ_2-3-NH_2py)$(H_2O)_4$]SO_4·H_2O (M = Ni and Co), the x- NH_2py ligand acts as a bridging ligand through the nitrogen donor atom from the pyridine and the nitrogen donor atom from the -NH_2 group [11]. Transition metal complex with py or x-NH_2py and the Cl^- ligands that have been synthesized tend to form monomeric structures, as shown in the complex [Zn(4-NH_2py)$_2Cl_2$] [4], [Cu(4-NH_2py)$_4$]Cl_2·$2CH_3OH$ [12], [Co(py)$_4Cl_2$] [13], and [Ni(py)$_2Cl_2$] [14].

Ni(II) complexes are important to study due to their potential as antibacterial agents [14], antifungal [15], antitumor [16], and catalyst [17], offering promising opportunities for further development as advanced materials. These complexes can exhibit coordination numbers of 4, 5, or 6 [18, 19]. A coordination number of 4 may lead to either square planar [20] or tetrahedral geometries [21], while a coordination number of 5 can result in trigonal bipyramidal [22] or square pyramidal geometries [23]. A coordination number of 6 typically forms an octahedral geometry [8, 9], which is the most commonly observed among Ni(II) complexes. Ni(II) complexes with aminopyridine have been successfully synthesized previously, including [Ni(4-NH_2py)$_2$(NCS)$_2$]$_n$ [8], [Ni(2-NH_2py)$_2$(NCS)$_2$]·$C_4H_{10}O$ [9], [Ni(3-NH_2py)$_2$(NCS)$_2$(H_2O)]·$2H_2O$ [9], and [Ni(4-NH_2py)$_2$(O_2CCH_3)$_2$(H_2O)$_2$] [10]. Complexes [8] and [10]

have been evaluated for their magnetic properties, exhibiting antiferromagnetic and paramagnetic behavior, respectively.

Previous studies have successfully synthesized compounds similar to the complex presented in this paper, such as $[Ni(py)_2Cl_2]$ [14]. Based on FT-IR, ^{13}C- NMR, and ^1H-NMR analyses, the reaction product was found to contain a mixture of two isomers: cis-$[Ni(py)_2Cl_2]$ and trans-$[Ni(py)_2Cl_2]$. Both complexes have been tested for antibacterial activity and demonstrated greater effectiveness than their corresponding free ligands. This suggests that the coordination bond between the metal center and the ligand plays a crucial role in enhancing antibacterial activity.

This article discusses the synthesis and characterization of the Ni(II) complex with the pyridine derivative (3-NH_2py), using a higher amount of the ligand. Based on the potential antibacterial properties of the 3-NH_2py ligand, a higher ligand concentration is expected to improve the complex's interaction with bacterial cell membranes and enhance antibacterial activity. Moreover, the presence of amine groups, which can directly interact with the bacterial membrane [24], is anticipated to further strengthen the antibacterial effect of the complex.

2. Experimental

2.1. Materials

$NiCl_2.6H_2O$ (Merck, 98%), 3-aminopyridine (Merck Millipore, 98%), and distilled water.

2.2. Procedures

2.2.1. Synthesis of the Complex $[Ni(3\text{-}NH_2py)_4Cl_2]$

The synthesis procedure for the complex $[Ni(3\text{-}NH_2py)_4Cl_2]$ refers to the research by Wijaya *et al.* [2], with some modifications to the solvent, temperature, and synthesis time. The synthesis was performed by reacting $NiCl_2.6H_2O$ (0.2377 g, 1 mmol) and 3-NH_2py (0.3764 g, 4 mmol) in water as the solvent for 1 hour at room temperature. Subsequently, the solution was placed in an autoclave and exposed to hydrothermal processing at 120°C for 4 hours. Then, the mixture was filtered, and the obtained filtrate was slowly evaporated. After 35 days, dark green crystals were formed (decomposition at 215°C).

2.2.2. Characterization Techniques

The complex compound was characterized using several tests, including melting point determination, electrical conductivity measurement, FT-IR analysis, and single-crystal XRD analysis. The melting point was measured using a Fisher-Johns Melting Point Apparatus at temperatures ranging from 28 to 350°C, with a heating rate of 20°C/min. Electrical conductivity was measured using a Cyberscan CON 11/110 conductometer in a methanol solvent at room temperature. FT-IR spectra were recorded on a Shimadzu IR Prestige-21 FTIR spectrometer over a wavenumber range of 500-4000 cm^{-1}. Crystal structure analysis was performed using a Bruker D8 Quest single-crystal XRD diffractometer.

2.2.3. Hirshfeld Surface Analysis

Hirshfeld surface analysis was performed using the CrystalExplorer software [25]. This analysis primarily serves to visualize intermolecular interactions on the crystal surface, facilitating understanding of crystal packing. The strength of the intermolecular interactions was mapped using a three-dimensional d_{norm} surface plotted on a fixed color scale ranging from 0.0870 (red) to 1.2944 (blue) [26]. The fingerprint plot was displayed using a distance range of 1.0-2.8 Å, with the distances d_i and d_e shown on the axes of the graph.

2.2.4. Antibacterial Test

The antibacterial activity of the complex compound was tested at the Integrated Laboratory of Universitas Negeri Malang, Indonesia, using the Kirby-Bauer agar diffusion method. The test was performed against *Escherichia coli* (ATCC 25922) and *Staphylococcus aureus* (ATCC 25923), with chloramphenicol as a positive control. A total of 10 mL of nutrient agar was poured into each petri dish, followed by the addition of 100 µL of bacterial suspension. The complex compound and reagents were dissolved in 10% dimethyl sulfoxide (DMSO) to a final concentration of 5 mg/mL. The prepared solutions were applied to sterile disks, which were then placed onto the agar surface. The plates were incubated at 37°C for 24 hours, after which the diameter of the inhibition zones was measured.

3. Results and Discussion

3.1. Synthesis of the Complex

The complex $[Ni(3\text{-}NH_2py)_4Cl_2]$ was synthesized by reacting $NiCl_2.6H_2O$ with the ligand 3-NH_2py in a 1:4 stoichiometric ratio using a hydrothermal method at 120°C for 4 hours. The crystal was obtained after slow evaporation over 35 days. The crystal form of $[Ni(3\text{-}NH_2py)_4Cl_2]$ exhibits notable differences from its starting materials: $NiCl_2.6H_2O$ appears as light green crystals, while 3-NH_2py forms dark brown needle-like crystals. In contrast, the synthesized complex forms flat dark green crystals (Figure 1), indicating the successful formation of a new compound distinct from the reactants. The reaction scheme for the formation of the complex is illustrated in Figure 1.

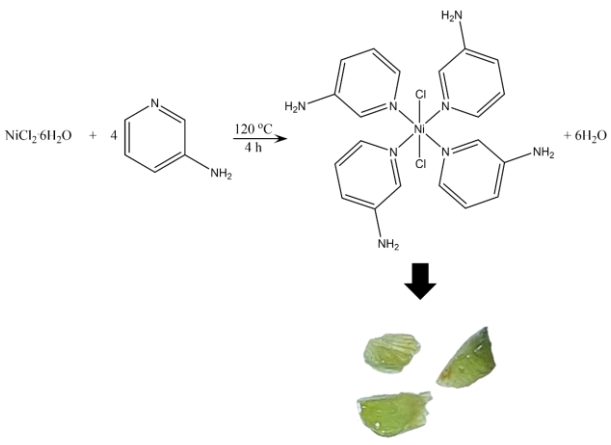

Figure 1. Formation reaction of $[Ni(3\text{-}NH_2py)_4Cl_2]$ complex

3.2. Characterization

3.2.1. Melting Point Determination

The melting point was determined to confirm the formation of a new compound distinct from its reactants. This indicates a reaction between the reactants, resulting in a new product that differs from the original materials [27]. The melting point data for the reactants and the synthesized compound are presented in Table 1.

As shown in Table 1, the synthesized complex exhibits a significantly higher melting point, accompanied by decomposition, which clearly differs from the melting points of the reactants. This provides further evidence for the successful formation of a new compound.

3.2.2. FT-IR Analysis

FT-IR analysis was conducted to determine the presence of the functional groups of the ligand 3-NH_2py in the complex. Peaks in the spectrum of the complex [Ni(3-NH_2py)$_4$Cl$_2$] at wavenumbers 1585 and 1293 cm^{-1} indicate the presence of the stretching vibrations of the aromatic groups C=N and C-NH_2, which are characteristic bonds in the pyridine ring [28, 29]. The symmetric and asymmetric stretching vibrations of the -NH_2 group are indicated by absorption bands at 3323 and 3380 cm^{-1}. A slight shift in the absorption band of the asymmetric - NH_2 stretching vibration from 3380 cm^{-1} to 3375 cm^{-1} may occur due to hydrogen bonding between the H atoms of the -NH_2 group and the Cl atoms of nearby molecules [30]. This minor shift suggests that the nitrogen atom of the $-NH_2$ group is not directly involved in coordination with the metal center.

Additionally, a significant shift is observed in the ring breathing mode. While the free 3-NH_2py ligand exhibits this vibration at 1015 cm^{-1}, it appears at 1023 cm^{-1} in the complex. This mode indicates coordination of the pyridine ring with the central ion through the nitrogen donor atom, reflected by the increase in wavenumber [31]. The interaction reduces the electron density on the nitrogen atom due to electron donation to the metal center, resulting in electron delocalization within the ring and a corresponding blue shift in the IR spectrum. Thus, it can be concluded that the nitrogen atom in the pyridine ring is involved in coordination. The FT-IR spectra of the complex [Ni(3-NH_2py)$_4$Cl$_2$] and the ligand 3-NH_2py are presented in Figure 2.

Table 1. Melting point data of the reactants and the synthesized complex [Ni(3-NH_2py)$_4$Cl$_2$]

Compound	Melting Point (°C)
$NiCl_2.6H_2O$	144-146
3-NH_2py	45-50
[Ni(3-NH_2py)$_4$Cl$_2$]	215-225*

*Decomposition

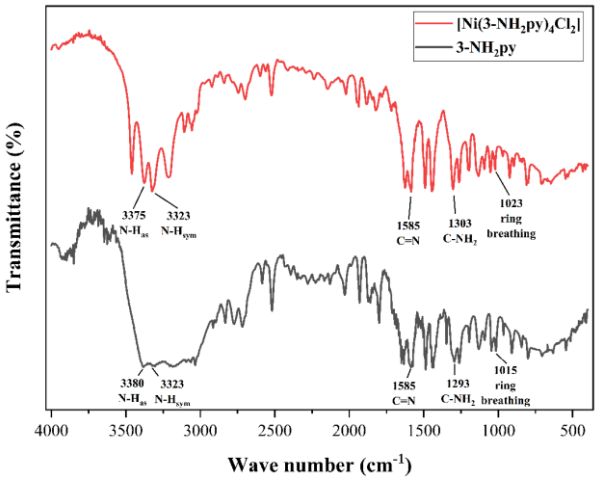

Figure 2. FT-IR spectra of the complex [Ni(3-NH_2py)$_4$Cl$_2$] and 3-NH_2py

3.2.3. Electrical Conductivity Test

The electrical conductivity test was conducted to evaluate whether the synthesized complex undergoes ionization or remains stable in solution. This test provides insight into the degree of ionization by measuring the number of molecular ions released into the solvent. A higher conductivity value indicates a greater degree of ionization, as the number of ions present in solution is directly proportional to the measured conductivity [32]. The electrical conductivity measurement of the complex (Table 2) shows a significant increase in conductivity for [Ni(3-NH_2py)$_4$Cl$_2$] compared to the pure solvent. However, its conductivity remains considerably lower than that of its constituent salts. This suggests the complex behaves as a weak electrolyte, undergoing partial ionization in water to produce [Ni(3-NH_2py)$_4$]$^{2+}$ and 2Cl^- ions.

3.2.4. Single-crystal XRD Analysis

The analysis of the [Ni(3-NH_2py)$_4$Cl$_2$] complex shows a coordination number of six with an octahedral geometry. The complex crystallizes in a triclinic system with the space group *P*$\bar{1}$. The coordination bonds in the complex occur between the central Ni(II) ion and four nitrogen atoms from the 3-NH_2py ligands. The 3-NH_2py acts as a monodentate ligand, coordinating to the central atom through the nitrogen donor atom of the pyridine ring in the equatorial position, while two Cl^- ligands occupy the axial positions (Figure 3). The crystallographic data for the complex can be seen in Table 3.

Table 2. Electrical conductivity of the solvent, reactant, and the complex

Compound	Concentration (mg/mL)	Electrical conductivity (µS/cm)
H_2O (solvent)	-	9.16
3-NH_2py	1	9.24
$NiCl_2.6H_2O$	1	934
[Ni(3-NH_2py)$_4$Cl$_2$]	1	468

Table 3. Crystallographic data of the complex [Ni(3-NH_2py)$_4Cl_2$]

Parameter	Value	
Chemical formula	$C_{20}H_{24}Cl_2N_8Ni$	
Molecular weight	506.08 g/mol	
Temperature	296.(2) K	
Wavelength	0.71073 Å	
Crystal system	Triclinic	
Space group	*P*$\bar{1}$	
Lattice parameters	a = 7.6428(8) Å	α = 73.920(4)°
	b = 8.5384(8) Å	β = 70.149(3)°
	c = 9.8610(13) Å	γ = 71.036(2)°
Volume	562.28(11)	
Z	1	
Type of X-ray radiation	Mo K\α	
Crystal size (mm)	0.21 × 0.2 × 0.15	
Absorption correction	Multi-Scan	
Number of reflections for determination	8359	
F(000)	262	
Density	1.495 g/cm^3	
Absorption coefficient	1.125 mm^{-1}	
h, k, l_{max}	9, 10, 12	
T_{min}, T_{max}	2.5683, 26.9528	
Data/Parameters/Restraints	2461/142/0	
R indices	R_1 = 0.0448, wR_2 = 0.0922	
CCDC number	2427099	

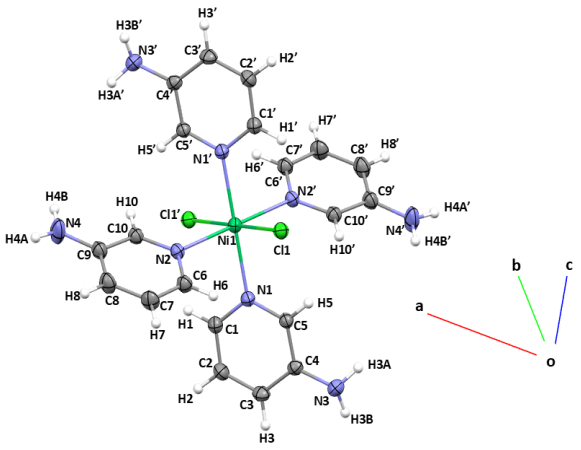

Figure 3. Structure of the complex [Ni(3-NH_2py)$_4Cl_2$]

The bond lengths between the Ni(II) metal ion and the nitrogen donor atoms of the 3-NH_2py ligand show only slight differences, as presented in Table 4. This is due to the repulsion occurring from the nitrogen atoms in the ligand, proven by the differences in the bond angles between the two nitrogen atoms through the central Ni(II) ion, as shown in Table 5.

The Ni-N bond length ranges from 2.157(3) to 2.166(3) Å. These values are not significantly different from the Ni–N bond length observed in the catena-[[Ni(μ_2-3-NH_2py)(H_2O)$_4$]SO_4.H_2O] complex, which is reported as 2.0979(17) Å [11]. The difference bond lengths between Ni-N1 (2.157(3) Å) and Ni-N2 (2.166(3) Å) is due to electron cloud repulsion among the ligands, as evidenced by the deviation in the dihedral angles between the rings of the 3-NH_2py ligand, specifically N1–Ni1–N2–C10 (51.63°) and N2–Ni1–N1 (55.82°). Additionally, the Ni–N bond lengths are shorter than the Ni–Cl bond lengths, which is likely due to the larger covalent radius of chlorine compared to nitrogen [4].

Based on the bond angle data in Table 5, the complex exhibits distortion, as indicated by the deviation of the bond angles from the normal octahedral angle [33]. The bond angle data of the nitrogen donor atoms through the central Ni(II) atom in the complex $[Ni(3\text{-}NH_2py)_4Cl_2]$ shows varying angles due to the repulsion between ligands, which leads to the formation of a stable complex with lower energy [4].

A single molecule of the $[Ni(3\text{-}NH_2py)_4Cl_2]$ complex is present within each unit cell of the crystal lattice, as shown in Figure 4. Several intermolecular interactions are observed, primarily involving N–H···Cl hydrogen bonds formed between the hydrogen atoms of the $-NH_2$ groups on the 3-NH_2py ligands and the chloride ligands of adjacent molecules (Figure 5).

Table 4. Bond length data around the central Ni(II) atom of the complex $[Ni(3\text{-}NH_2py)_4Cl_2]$

Interatomic bonds	Bond length (Å)
Ni1-N1	2.157(3)
Ni1-N2	2.166(3)
Ni1-Cl1	2.4757(8)
Ni1-N1'	2.157(3)
Ni1-N2'	2.166(3)
Ni1-Cl1'	2.4757(8)

Table 5. Bond angle data of the two nitrogen atoms passing through the central Ni(II) atom of the complex $[Ni(3\text{-}NH_2py)_4Cl_2]$

Angle between atoms	Bond angle (°)
N1-Ni1-N1'	180.00
N1'-Ni1-N2	95.31(10)
N1-Ni1-N2	84.69(10)
N1'-Ni1-N2'	84.69(10)
N1-Ni1-N2'	95.31(10)
N1-Ni1-Cl1'	90.35(7)
N1'-Ni1-Cl1'	89.65(7)
N2-Ni1-Cl1	89.92(7)
N2-Ni1-Cl1'	90.08(7)
N1'-Ni1-Cl1'	89.65(7)
N1'-Ni1-Cl1	90.35(7)
N2'-Ni1-Cl1	90.08(7)
N2'-Ni1-Cl1'	89.92(7)
Cl1-Ni1-Cl1'	180.00

3.2.5. Hirshfeld Surface Analysis

Hirshfeld surface analysis was performed using the CrystalExplorer software [25]. This analysis is used to visualize intermolecular interactions quantitatively. It also includes a fingerprint plot feature to identify interactions between atoms. The strength of intermolecular interactions is mapped using a three-dimensional d_{norm} surface, plotted on a fixed color scale from 0.0870 (red) to 1.2944 (blue) [26]. The d_{norm} values on the Hirshfeld surface are mapped using red, blue, and white colors. Blue regions represent positive d_{norm} values, while white regions indicate d_{norm} = 0, signifying that the interaction distances equal the sum of the van der Waals radii. Dark red spots indicate the presence of hydrogen bonds with neighboring molecules, and other intermolecular interactions are represented by bright red dots [34].

The three-dimensional d_{norm} surface of the complex is shown in Figure 6(a). The red areas around the H atoms (from the -NH_2 group) indicate intermolecular interactions between the H atoms with the Cl ligands and the H atoms from the pyridine ring of nearby molecules. The red areas around the Cl ligands show interactions between the Cl^- ligands and the H atoms (from the -NH_2 group) of the 3-NH_2py ligands from the nearest complex. Additionally, there are weak interactions between the H atoms of the pyridine ring and the H atoms (from the -NH_2 group) of the 3-NH_2py ligands.

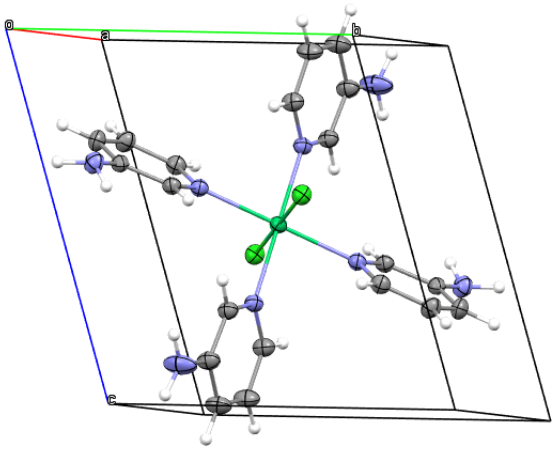

Figure 4. The complex $[Ni(3\text{-}NH_2py)_4Cl_2]$ within a crystal lattice

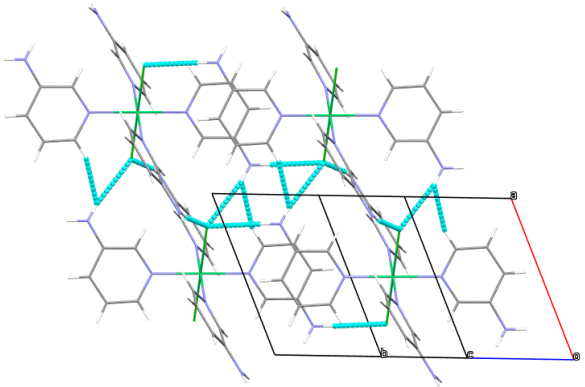

Figure 5. Intermolecular interactions in crystal packing

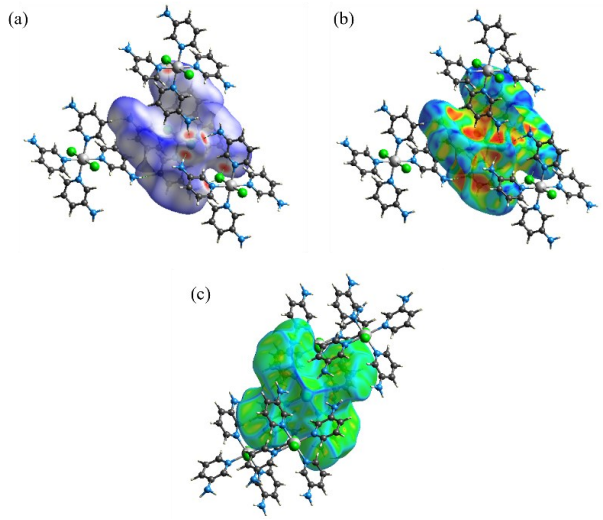

Figure 6. (a) Results of the d_{norm} analysis, (b) shape index, and (c) curvedness

The shape index map of the $[Ni(3\text{-}NH_2py)_4Cl_2]$ complex (Figure 6(b)) illustrates the donor and acceptor groups involved in intermolecular interactions [35]. Red regions surrounding certain atoms indicate their role as acceptors, while blue regions signify donor atoms. Based on this analysis, the Cl^- ligands act as acceptors, whereas the hydrogen atoms of the $-NH_2$ groups serve as donors in the observed interactions.

The curvedness map (Figure 6(c)) highlights variations in the crystal surface topology, where green regions indicate relatively flat surfaces and blue regions represent curved areas of the molecular surface [36]. The flat regions are predominantly located in the 3-NH_2py ring area, likely due to $\pi-\pi$ stacking interactions, where the contact distances are nearly identical. This suggests a high degree of planarity and close packing in these regions, which may contribute to the stability of the crystal structure. The blue lines on the curvedness map delineate the molecular shape and indicate the contact areas between adjacent molecules [37].

The two-dimensional fingerprint plot serves to provide quantitative information about the properties and types of intermolecular contacts among the molecules in the crystal packing [34, 36]. The displayed fingerprint plot uses a range of 1.0-2.8 Å, with the distance scale shown on the graph's axes. The symbol d_i represents the distance from the Hirshfeld surface to the nearest interior atom within the Hirshfeld surface, while d_e indicates the distance from the Hirshfeld surface to the nearest exterior atom outside the Hirshfeld surface [35]. The interatomic contacts significantly contributing to the crystal packing are H---H, C---H, H---Cl, and N---H, with respective percentage values of 50.9%, 20.0%, 13.5%, and 9.0%. Other interatomic contacts that contribute weakly to the crystal packing are C---C and C---N, with percentage values of 5.5% and 1.1%, respectively. The fingerprint plot of the interatomic contacts in the complex compound is presented in Figure 7.

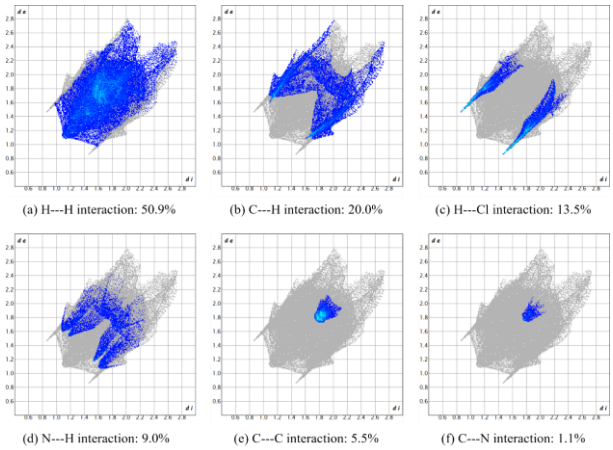

Figure 7. Individual atom interactions in crystal packing

3.2.6. Antibacterial Activity

The measurement of the inhibition zone diameter showed that the complex exhibited antibacterial activity against gram-positive bacteria (*S. aureus*) and gram-negative bacteria (*E. coli*), with inhibition zone diameters as shown in Table 6. The antibacterial data of the complex compared to its free ligand showed a significant increase. The antibacterial activity is likely due to the interaction between the 3-NH_2py ligand and the bacterial cell membrane through hydrogen bonding [1, 38]. The interaction of the metal complex with the cell membrane disrupts normal physiological and chemical functions essential for bacterial cell survival.

The Ni(II) ion also acts as a catalyst for oxidizing certain peptide side chains and inhibits bacterial cell activity. The redox properties of the metal complex can generate reactive oxygen species and hydrolyze phosphoester bonds, damaging DNA and preventing enzyme activity essential for cell growth [39, 40, 41]. However, the antibacterial activity of the $[Ni(3\text{-}NH_2py)_4Cl_2]$ complex is lower compared to the positive control, chloramphenicol. Therefore, further optimization is required, either by testing the complex at varying concentrations to enhance its efficacy or by substituting the Cl^- ligand with another ligand that may exhibit stronger interactions with the bacterial cell membrane, thereby increasing antibacterial activity.

Table 6. The diameter of the inhibition zones of the ligand, metal salt, and complex

Compounds	Inhibition zone (mm)	
	S. aureus	*E. coli*
$NiCl_2{\cdot}6H_2O$	7.10	7.20
3-NH_2py	0.00	0.00
$[Ni(3\text{-}NH_2py)_4Cl_2]$	6.90	6.90
Chloramphenicol (+)	22.32	21.85
DMSO 10% (-)	0.00	0.00

4. Conclusion

[Ni(3-NH_2py)Cl_2] complex was successfully synthesized using the hydrothermal method at 120°C for 4 hours. The complex decomposes at 215°C and is classified as a weak ionic compound. FT-IR analysis reveals the presence of characteristic functional groups of the ligand 3-NH_2py. The complex crystallizes with a distorted octahedral geometry and has a triclinic structure with space group $P\bar{1}$ (a = 7.6428(8) Å, b = 8.5384(8) Å, c = 9.8610(13) Å, α = 73.920(4)°, β = 70.149(3)°, γ = 71.036(2)°). Hirshfeld surface analysis indicates the presence of intermolecular N-H---Cl interactions, with H---H atom interactions contributing most significantly to the packing at a percentage of 50.9%. The increased antibacterial activity of the complex is due to the interaction between the ligand and the bacterial cell membrane and the active role of Ni(II) in killing bacteria through membrane cell damage.

Acknowledgments

Many thanks were delivered to Universitas Negeri Malang through the Institute of Research and Community Service (LPPM) for funding the PNBP grant scheme for this research with contract number 4.4.607/UN32.14.1/LT/2024.

References

[1] Orie Kingsley John, Duru Remy Ukachukwu, I. oro Ngochindo Raphael, Syntheses, Complexation and Biological Activity of Aminopyridines: A Mini-Review, *American Journal of Heterocyclic Chemistry*, 7, 2, (2021), 11-25 https://doi.org/10.11648/j.ajhc.20210702.11

[2] Husni Wahyu Wijaya, Galih Candra Nugraha, Viona Dinda Alfian, Ubed Sonai Fahruddin Arrozi, Meyga Evi Ferama Sari, Sutandyo Dwija Laksmana, Faaza'izzahaq Setta Putra, I. Wayan Dasna, Synthesis, structure, hirshfeld surface analysis and antibacterial activities of [Cd(2-ampy)$_3$(NCS)($\mu_{1,5}$-SCN)]$_2$ and [Cd(4-ampy)$_2$($\mu_{1,5}$-dca)$_2$]$_n$ complexes (2-ampy = 2-aminopyridine, 4-ampy = 4-aminopyridine, NCS = thiocyanate, dca = dicyanamide), *Chemistry of Inorganic Materials*, 3, (2024), 100054 https://doi.org/10.1016/j.cinorg.2024.100054

[3] Linggar Agil Savitri, Faaza'izzahaq Setta Putra, Sutandyo Dwija Laksmana, Dewi Mariyam, I Wayan Dasna, Synthesis, Structure, Antibacterial Activity, and Hirshfeld Surface Analysis of Complex [Co(4-ampy)$_4$(NCS)$_2$]·CO_2, *Indonesian Journal of Chemistry*, 24, 4, (2024), 1046-1057 https://doi.org/10.22146/ijc.90585

[4] I Wayan Dasna, Dewi Mariyam, Husni Wahyu Wijaya, Ubed Sonai Fahruddin Arrozi, Sugiarto Sugiarto, Synthesis, Structural Determination and Antibacterial Properties of Zinc(II) Complexes Containing 4-Aminopyridine Ligands, *Indonesian Journal of Chemistry*, 23, 4, (2023), 1108-1119 https://doi.org/10.22146/ijc.82801

[5] M. E. Moustafa, N. M. Meshal, M. I. Ayad, O. A. Goda, Aminopyridine Transition Metals Complexes; Characterization, Application and Molecular Orbital Calculation, *Benha Journal of Applied Sciences*, 5, 7, (2020), 231-243 https://doi.org/10.21608/bjas.2020.228550

[6] Brina Dojer, Andrej Pevec, Marko Jagodič, Matjaž Kristl, Miha Drofenik, Three new cobalt(II) carboxylates with 2-, 3- and 4-aminopyridine: Syntheses, structures and magnetic properties, *Inorganica Chimica Acta*, 383, (2012), 98-104 https://doi.org/10.1016/j.ica.2011.10.056

[7] Muhammad Hafeez, Muhammad Riaz, Aminopyridine stabilized group-IV metal complexes and their applications, *Applied Petrochemical Research*, 6, 4, (2016), 307-340 https://doi.org/10.1007/s13203-016-0170-1

[8] Tristan Neumann, Magdalena Ceglarska, Luzia S. Germann, Michał Rams, Robert E. Dinnebier, Stefan Suckert, Inke Jess, Christian Näther, Structures, Thermodynamic Relations, and Magnetism of Stable and Metastable Ni(NCS)$_2$ Coordination Polymers, *Inorganic Chemistry*, 57, 6, (2018), 3305-3314 https://doi.org/10.1021/acs.inorgchem.8b00092

[9] Madeleine H. Moore, Luigi R. Nassimbeni, Margaret L. Niven, Studies in Werner Clathrates. Part 6. Structures of two novel polymeric inclusion compounds: poly(bis(isothiocyanato)di(2-aminopyridine)nickel(II)) • diethylether and di(aqua bis(isothiocyanato)3-aminopyridine μ-3-aminopyridine nickel(II))·water, *Inorganica Chimica Acta*, 132, 1, (1987), 61-66 https://doi.org/10.1016/S0020-1693(00)83990-0

[10] Brina Dojer, Amalija Golobič, Zvonko Jagličić, Matjaž Kristl, Miha Drofenik, Two new nickel(II) carboxylates with 3- and 4-aminopyridine: syntheses, structures, and magnetic properties, *Monatshefte für Chemie - Chemical Monthly*, 143, 1, (2012), 73-78 https://doi.org/10.1007/s00706-011-0578-3

[11] Franz A. Mautner, Patricia V. Jantscher, Roland C. Fischer, Ana Torvisco, Klaus Reichmann, Salah S. Massoud, Syntheses, structural characterization, and thermal behaviour of metal complexes with 3-aminopyridine as co-ligands, *Transition Metal Chemistry*, 46, 3, (2021), 191-200 https://doi.org/10.1007/s11243-020-00436-2

[12] Bojidarka B. Ivanova, Heike and Mayer-Figge, Crystal structure and solid state IR-LD analysis of a mononuclear Cu(II) complex of 4-aminopyridine, *Journal of Coordination Chemistry*, 58, 8, (2005), 653-659 https://doi.org/10.1080/00958970412331336295

[13] Bahar Molaei, Seyed Abolghasem Kahani, Synthesis of cobalt-based magnetic nanocrystals from cobalt(II) heterocyclic amine complexes, *Research on Chemical Intermediates*, 43, 4, (2017), 2627-2640 https://doi.org/10.1007/s11164-016-2785-3

[14] Faridul Islam, Md. Amran Hossain, Nur Mostaq Shah, Hridika Talukder Barua, Md. Alamgir Kabir, Mohammad Jamshed Khan, Romel Mullick, Synthesis, Characterization, and Antimicrobial Activity Studies of Ni(II) Complex with Pyridine as a Ligand, *Journal of Chemistry*, 2015, 1, (2015), 525239 https://doi.org/10.1155/2015/525239

[15] Pushap Raj, Amanpreet Singh, Ajnesh Singh, Narinder Singh, Syntheses and Photophysical Properties of Schiff Base Ni(II) Complexes: Application for Sustainable Antibacterial Activity

and Cytotoxicity, *ACS Sustainable Chemistry & Engineering*, 5, 7, (2017), 6070-6080 https://doi.org/10.1021/acssuschemeng.7b00963

[16] Heba Alshater, Ahlam I. Al-Sulami, Samar A. Aly, Ehab M. Abdalla, Mohamed A. Sakr, Safaa S. Hassan, Antitumor and Antibacterial Activity of Ni(II), Cu(II), Ag(I), and Hg(II) Complexes with Ligand Derived from Thiosemicarbazones: Characterization and Theoretical Studies, *Molecules*, 28, 6, (2023), 2590 https://doi.org/10.3390/molecules28062590

[17] Biyun Su, Yiting Liu, Tingyu Yan, Jindi Wu, Qiaoqiao Han, Li Wang, Liangtao Ran, Dandan Pan, Nickel(II) complexes with mono(imino)pyrrole ligands: preparation, structure, DFT calculation and catalytic behavior, *Transition Metal Chemistry*, 46, 8, (2021), 601-611 https://doi.org/10.1007/s11243-021-00478-0

[18] Jack Ghannam, Talal Al Assil, Trey C. Pankratz, Richard L. Lord, Matthias Zeller, Wei-Tsung Lee, A Series of 4- and 5-Coordinate Ni(II) Complexes: Synthesis, Characterization, Spectroscopic, and DFT Studies, *Inorganic Chemistry*, 57, 14, (2018), 8307-8316 https://doi.org/10.1021/acs.inorgchem.8b00958

[19] Mithun Chakrabarty, Aziz Ahmed, R. A. Lal, Synthesis, Characterization, and Structural Assessment of Ni(II) Complexes Derived from Bis(2-hydroxy-1-naphthaldehyde)succinoyldihydrazone, *International Journal of Inorganic Chemistry*, 2015, 1, (2015), 121895 https://doi.org/10.1155/2015/121895

[20] Dominik Lomjanský, Cyril Rajnák, Ján Titiš, Ján Moncoľ, Lukáš Smolko, Roman Boča, Impact of tetrahedral and square planar geometry of Ni(II) complexes with (pseudo)halide ligands to magnetic properties, *Inorganica Chimica Acta*, 483, (2018), 352-358 https://doi.org/10.1016/j.ica.2018.08.029

[21] M. Gerloch, L. R. Hanton, M. R. Manning, Tetrahedral complexes of nickel(II): Electronic spectra, σ and π bonding, and the electroneutrality principle, *Inorganica Chimica Acta*, 49, (1981), 139 https://doi.org/10.1016/S0020-1693(00)90472-9

[22] Divya Sasi, Venkatachalam Ramkumar, Narasimha N. Murthy, Bite-Angle-Regulated Coordination Geometries: Tetrahedral and Trigonal Bipyramidal in Ni(II) with Biphenyl-Appended (2-Pyridyl)alkylamine *N*,*N*′-Bidentate Ligands, *ACS Omega*, 2, 6, (2017), 2474-2481 https://doi.org/10.1021/acsomega.7b00119

[23] Rezan A. Saleh, Hikmat A. Mohamad, Muhammad Ashfaq, Subhi A. Al-Jibori, Muhammad Nawaz Tahir, A Slightly Distorted Square Pyramidal Nickel(II) Complex: Synthesis, Characterizations, X-ray Crystal Structure, Anticancer Activity, Electrochemistry, DFT and Hirshfeld Surface Studies of $[NiCl(dppe)_2]Cl.CH_2Cl_2$, dppe: 1,2-Bis(Diphenylphosphino)Ethane, *Chemistry Africa*, 7, 8, (2024), 4261-4271 https://doi.org/10.1007/s42250-024-01039-5

[24] Hatsuo Yamamura, Tatsuya Hagiwara, Yuma Hayashi, Kayo Osawa, Hisato Kato, Takashi Katsu, Kazufumi Masuda, Ayumi Sumino, Hayato Yamashita, Ryo Jinno, Masayuki Abe, Atsushi Miyagawa, Antibacterial Activity of Membrane-Permeabilizing Bactericidal Cyclodextrin Derivatives, *ACS Omega*, 6, 47, (2021), 31831-31842 https://doi.org/10.1021/acsomega.1c04541

[25] Peter R. Spackman, Michael J. Turner, Joshua J. McKinnon, Stephen K. Wolff, Daniel J. Grimwood, Dylan Jayatilaka, Mark A. Spackman, CrystalExplorer: a program for Hirshfeld surface analysis, visualization and quantitative analysis of molecular crystals, *Journal of Applied Crystallography*, 54, 3, (2021), 1006-1011 https://doi.org/10.1107/S1600576721002910

[26] Cemile Baydere, Merve Taşçı, Necmi Dege, Mustafa Arslan, Yusuf Atalay, Irina A. Golenya, Crystal structure and Hirshfeld surface analysis of (*E*)-2-(2, 4, 6-trimethylbenzylidene)-3, 4-dihydronaphthalen-1 (2*H*)-one, *Acta Crystallographica Section E Crystallographic Communications*, 75, 6, (2019), 746-750 https://doi.org/10.1107/S2056989019006182

[27] Dewi Mariyam, Nani Farida, Husni Wahyu Wijaya, I. Wayan Dasna, Studi Karakterisasi dan Aktivitas Antibakteri Senyawa Kompleks dari Zink(II) Klorida, Kalium Tiosianat dan 2-Aminopiridina, *Jurnal Riset Kimia*, 13, 1, (2022), 100-110 https://doi.org/10.25077/jrk.v13i1.465

[28] Zeki Kartal, Onur ŞAHİN, The synthesis of heteroleptic cyanometallate aminopyridine complexes and an investigation into their structural properties with various spectroscopic methods, *Journal of Molecular Structure*, 1227, (2021), 129514 https://doi.org/10.1016/j.molstruc.2020.129514

[29] Asmi Munadhiroh, Husni Wahyu Wijaya, Nani Farida, Stéphane Golhen, I Wayan Dasna, Synthesis, Characterization, and Preliminary Study of $[Co(2\text{-aminopyridine})_2(NCS)_2]$ or bis (2-aminopyridine) dithiocyanato cobalt (II) as An Antibacterial, *Jurnal Kimia Valensi*, 8, 1, (2022), 23-29 https://doi.org/10.15408/jkv.v8i1.22685

[30] Poul Erik Hansen, Mohammad Vakili, Fadhil S. Kamounah, Jens Spanget-Larsen, NH Stretching Frequencies of Intramolecularly Hydrogen-Bonded Systems: An Experimental and Theoretical Study, *Molecules*, 26, 24, (2021), 7651 https://doi.org/10.3390/molecules26247651

[31] Y. Buyukmurat, S. Akyuz, Theoretical and experimental studies of IR spectra of 4-aminopyridine metal(II) complexes, *Journal of Molecular Structure*, 651-653, (2003), 533-539 https://doi.org/10.1016/S0022-2860(02)00674-9

[32] Moamen S. Refat, Ibrahim M. El-Deen, Mohamed A. Zein, Abdel Majid A. Adam, Mohamed I. Kobeasy, Spectroscopic, Structural and Electrical Conductivity Studies of Co(II), Ni(II) and Cu(II) Complexes derived from 4-Acetylpyridine with Thiosemicarbazide, *International Journal of Electrochemical Science*, 8, 7, (2013), 9894-9917 https://doi.org/10.1016/S1452-3981(23)13021-5

[33] R. J. Gillespie, Bond Lengths and Bond Angles in Octahedral, Trigonal-Bipyramidal, and Related Molecules of The Non-Transition Elements, *Canadian Journal of Chemistry*, 39, 2, (1961), 318-323 https://doi.org/10.1139/v61-037

[34] Ferdaousse Rhoufal, Abdelhakim Laachir, Salaheddine Guesmi, Laurent Jouffret, Nicolas Sergent, Saïd Obbade, Mehmet Akkurt, Fouad Bentiss, New Cobalt(II) and Copper(II) Thiocyanate Complexes of 2,5-Bis(pyridin-2-yl)-1,3,4-oxadiazole Ligand: Synthesis, Crystal Structures, Spectral Properties and Hirshfeld Surface Analysis,

ChemistrySelect, 4, 26, (2019), 7773-7783 https://doi.org/10.1002/slct.201901219

[35] Muhammad Ashfaq, Khurram Shahzad Munawar, Muhammad Nawaz Tahir, Necmi Dege, Mavise Yaman, Shabbir Muhammad, Saleh S. Alarfaji, Hadi Kargar, Muhammad Umar Arshad, Synthesis, Crystal Structure, Hirshfeld Surface Analysis, and Computational Study of a Novel Organic Salt Obtained from Benzylamine and an Acidic Component, *ACS Omega*, 6, 34, (2021), 22357-22366 https://doi.org/10.1021/acsomega.1c03078

[36] Khaoula Azouzi, Besma Hamdi, Ridha Zouari, Abdelhamid Ben Salah, Synthesis, structure and Hirshfeld surface analysis, vibrational and DFT investigation of (4-pyridine carboxylic acid) tetrachlorocuprate (II) monohydrate, *Bulletin of Materials Science*, 40, 2, (2017), 289-299 https://doi.org/10.1007/s12034-017-1375-3

[37] Saikat Kumar Seth, Debayan Sarkar, Amalesh Roy, Tanusree Kar, Insight into supramolecular self-assembly directed by weak interactions in acetophenone derivatives: crystal structures and Hirshfeld surface analyses, *CrystEngComm*, 13, 22, (2011), 6728-6741 https://doi.org/10.1039/C1CE05670K

[38] Konstantina Karathanou, Ana-Nicoleta Bondar, Dynamic Water Hydrogen-Bond Networks at the Interface of a Lipid Membrane Containing Palmitoyl-Oleoyl Phosphatidylglycerol, *The Journal of Membrane Biology*, 251, 3, (2018), 461-473 https://doi.org/10.1007/s00232-018-0023-1

[39] K. Bazaka, M. V. Jacob, W. Chrzanowski, K. Ostrikov, Anti-bacterial surfaces: natural agents, mechanisms of action, and plasma surface modification, *RSC Advances*, 5, 60, (2015), 48739-48759 https://doi.org/10.1039/C4RA17244B

[40] Baskaran Ramalingam, Thanusu Parandhaman, Sujoy K. Das, Antibacterial Effects of Biosynthesized Silver Nanoparticles on Surface Ultrastructure and Nanomechanical Properties of Gram-Negative Bacteria viz. *Escherichia coli* and *Pseudomonas aeruginosa*, *ACS Applied Materials & Interfaces*, 8, 7, (2016), 4963-4976 https://doi.org/10.1021/acsami.6b00161

[41] Sriatun Sriatun, Khairini Pertiwi, Choiril Azmiyawati, Mukhammad Asyari, Damar Nurwahyu Bima, Nor Aida Zubir, Enhanced Antibacterial Efficacy of Ag(I), Cu(II), and Zn(II) Modified Sodalite Zeolite Against *Escherichia coli* and *Staphylococcus aureus*, *Jurnal Kimia Sains dan Aplikasi*, 27, 10, (2024), 477-484 https://doi.org/10.14710/jksa.27.10.477-484